International Workshop XLI on Gross Properties of Nuclei and Nuclear Excitations,
"Astrophysics and Nuclear Structure", Jan 26 – Feb 1, 2013, Hirschegg, Austria

Self-consistent description of supernova electron capture and neutrino-nucleus processes

N. Paar

Physics Department
Faculty of Science
University of Zagreb
Croatia

OUTLINE

The goal is self-consistent microscopic description inspired by EDFs, of nuclear structure, excitations, weak interaction processes, and nuclear equation of state of relevance for astrophysics and nucleosynthesis

1. Inelastic neutrino-nucleus reactions involving supernova neutrinos. Large-scale calculations for charge-exchange reactions

2. Electron capture on nuclei at finite temperature in stellar environment

3. Nuclear equation of state – constraints on the symmetry energy from theory of collective nuclear motion and experimental data

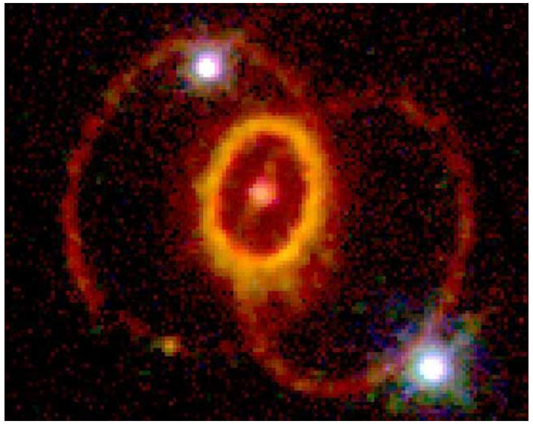

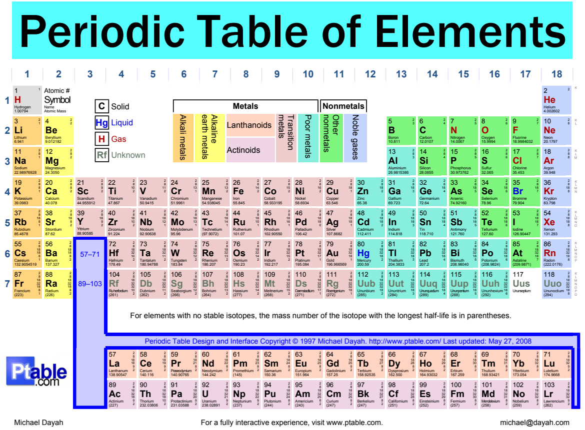

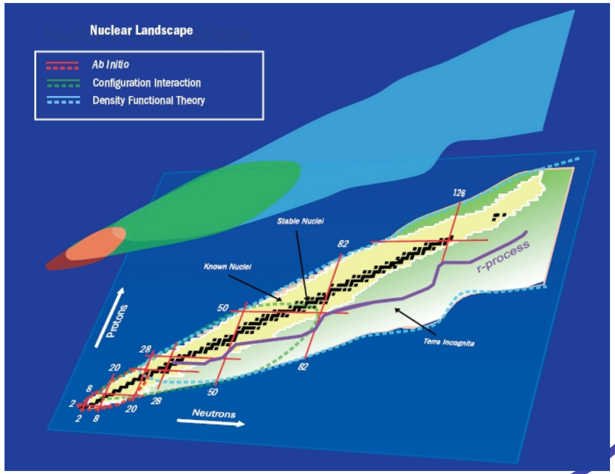

LOW-ENERGY NEUTRINO-NUCLEUS PROCESSES

Charged-current neutrino-nucleus reactions

$$\nu_l +_Z X_N \rightarrow_{Z+1} X^*_{N-1} + l^-$$

$$\bar{\nu}_l +_Z X_N \rightarrow_{Z-1} X^*_{N+1} + l^+$$

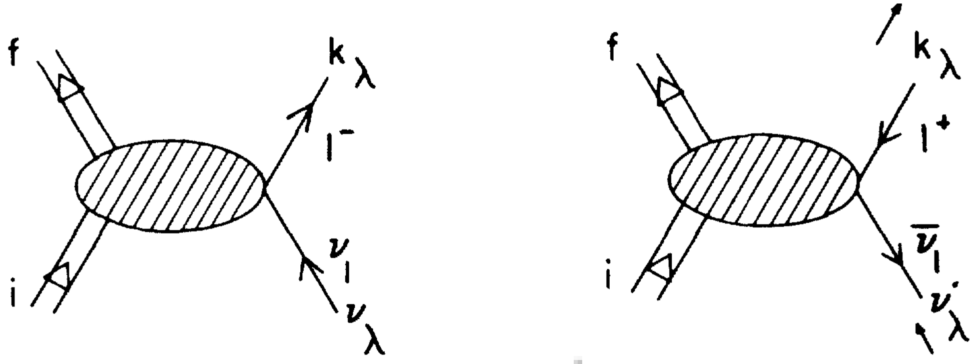

The properties of nuclei and their excitations govern the neutrino-nucleus cross sections. Nuclear transitions induced by neutrinos involve operators with finite momentum transfer.

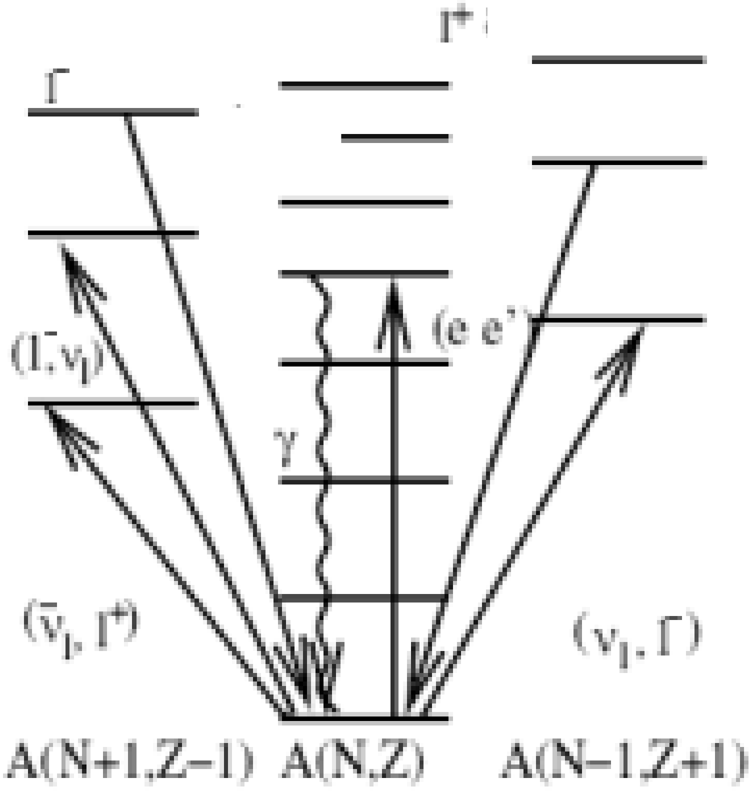

NEUTRINO-NUCLEUS CROSS SECTIONS

$$\frac{d\sigma_\nu}{d\Omega} = \frac{2G_F^2 cos^2\theta_c}{\pi}\frac{E_l^2}{2J_i+1}$$

$$\times \left\{ \sum_{J\geq 1} \left\{ [1-(\hat{\boldsymbol{\nu}}\cdot\hat{\boldsymbol{q}})(\hat{\boldsymbol{q}}\cdot\boldsymbol{\beta})] \left[|\langle J_f||\hat{\mathcal{T}}_J^{MAG}||J_i\rangle|^2 + |\langle J_f||\hat{\mathcal{T}}_J^{EL}||J_i\rangle|^2 \right] \right. \right.$$

$$+[\hat{\boldsymbol{q}}(\hat{\boldsymbol{\nu}}-\boldsymbol{\beta})] 2Re\langle J_f||\hat{\mathcal{T}}_J^{MAG}||J_i\rangle\langle J_f||\hat{\mathcal{T}}_J^{EL}||J_i\rangle^* \Big\}$$

$$+ \sum_{J\geq 0} \left\{ (1+\hat{\boldsymbol{\nu}}\cdot\boldsymbol{\beta})|\langle J_f||\hat{\mathcal{M}}_J||J_i\rangle|^2 \right.$$

$$+(1-\hat{\boldsymbol{\nu}}\cdot\boldsymbol{\beta}+2(\hat{\boldsymbol{\nu}}\cdot\hat{\boldsymbol{q}})(\hat{\boldsymbol{q}}\cdot\boldsymbol{\beta}))|\langle J_f||\hat{\mathcal{L}}_J||J_i\rangle|^2$$

$$-[\hat{\boldsymbol{q}}(\hat{\boldsymbol{\nu}}+\boldsymbol{\beta})] 2Re\langle J_f||\hat{\mathcal{L}}_J||J_i\rangle\langle J_f||\hat{\mathcal{M}}_J||J_i\rangle^* \Big\}\Big\}$$

$$\boldsymbol{k} = E_l\boldsymbol{\beta}$$

Transition matrix elements are described in a self-consistent way using relativistic Hartree-Bogoliubov model for the initial (ground) state and relativistic quasiparticle random phase approximation for excited states (RHB+RQRPA)

DD-ME2 density-dependent effective interaction + Gogny pairing

CHARGED-CURRENT NEUTRINO-NUCLEUS CROSS SECTIONS

Multipole composition of the neutrino-nucleus cross sections:
RNEDF (DD-ME2) vs. shell model + RPA (SGII)

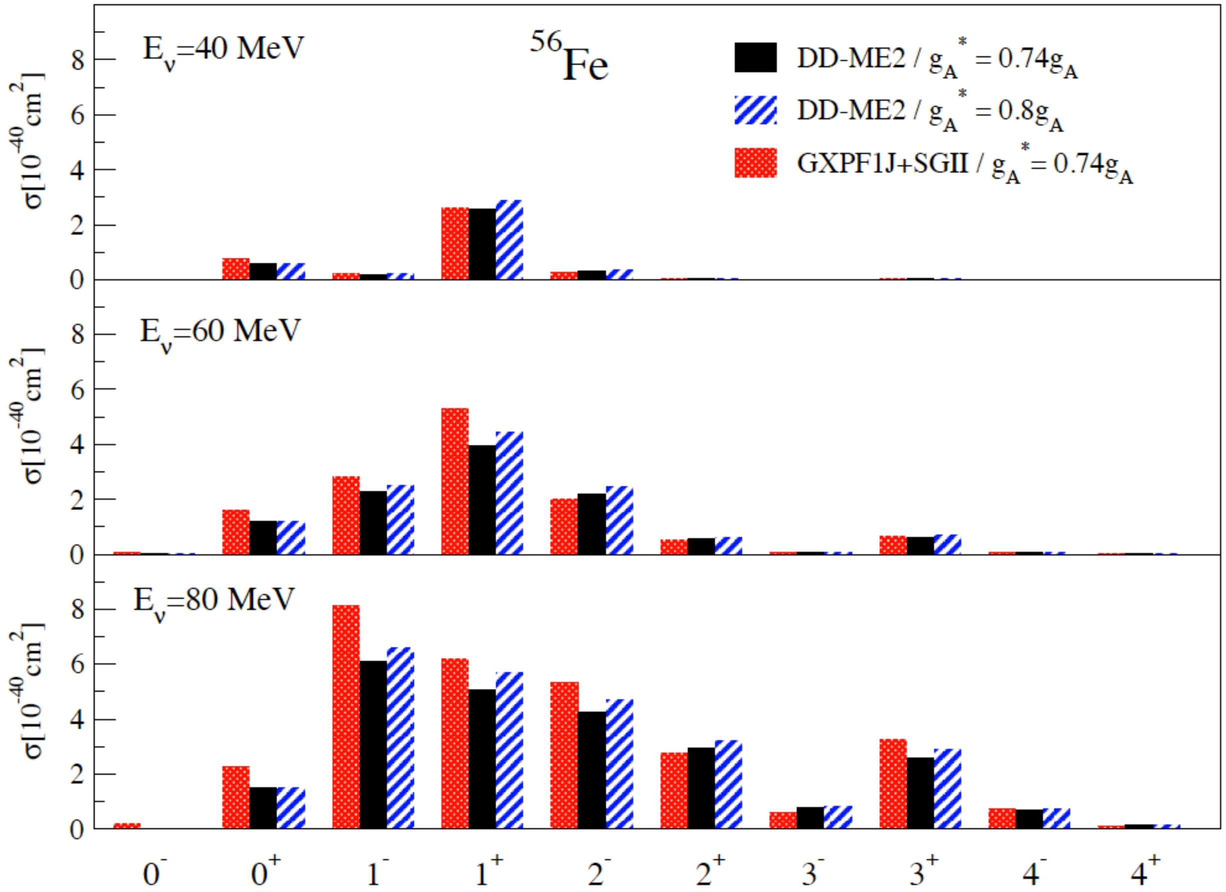

In addition to GT, at larger neutrino energies exitations of higher multipolarities (forbidden transitions) contribute.

Remarkable agreement between models based on completely different foundations and effective interactions !

UNCERTAINTIES IN MODELING ν-NUCLEUS CROSS SECTIONS

Neutrino-nucleus cross sections for ^{56}Fe target, averaged over the electron neutrino from μ^+ decay at rest (DAR)

$^{56}Fe(\nu_e,e^-)\,^{56}Co$	<σ>(10^{-42}cm^2)
QRPA(SIII) (Lazauskas et al.)	352
Shell model (GXPF1J) + RPA (SGII) (T. Suzuki et al.)	259
RPA (Kolbe, Langanke)	240
QRPA (Cheoun et al.)	173
RNEDF (DD-ME2)	263
EXP. (KARMEN)	256±108±43

$$\langle\sigma_\nu\rangle = \frac{\int dE_\nu \sigma_\nu(E_\nu) f(E_\nu)}{\int dE'_\nu f(E'_\nu)}$$

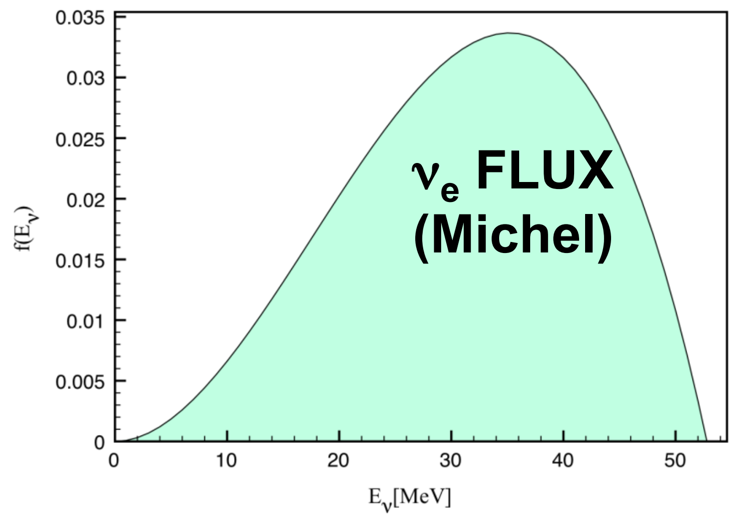

$$\langle\sigma\rangle_{th} = (258 \pm 57) \times 10^{-42} cm^2$$

Present theoretical uncertainty from all models appear considerably smaller than the experimental one.

LARGE-SCALE CALCULATIONS OF ν_e-NUCLEUS CROSS SECTIONS

The cross sections are averaged over the neutrino spectrum from muon DAR.

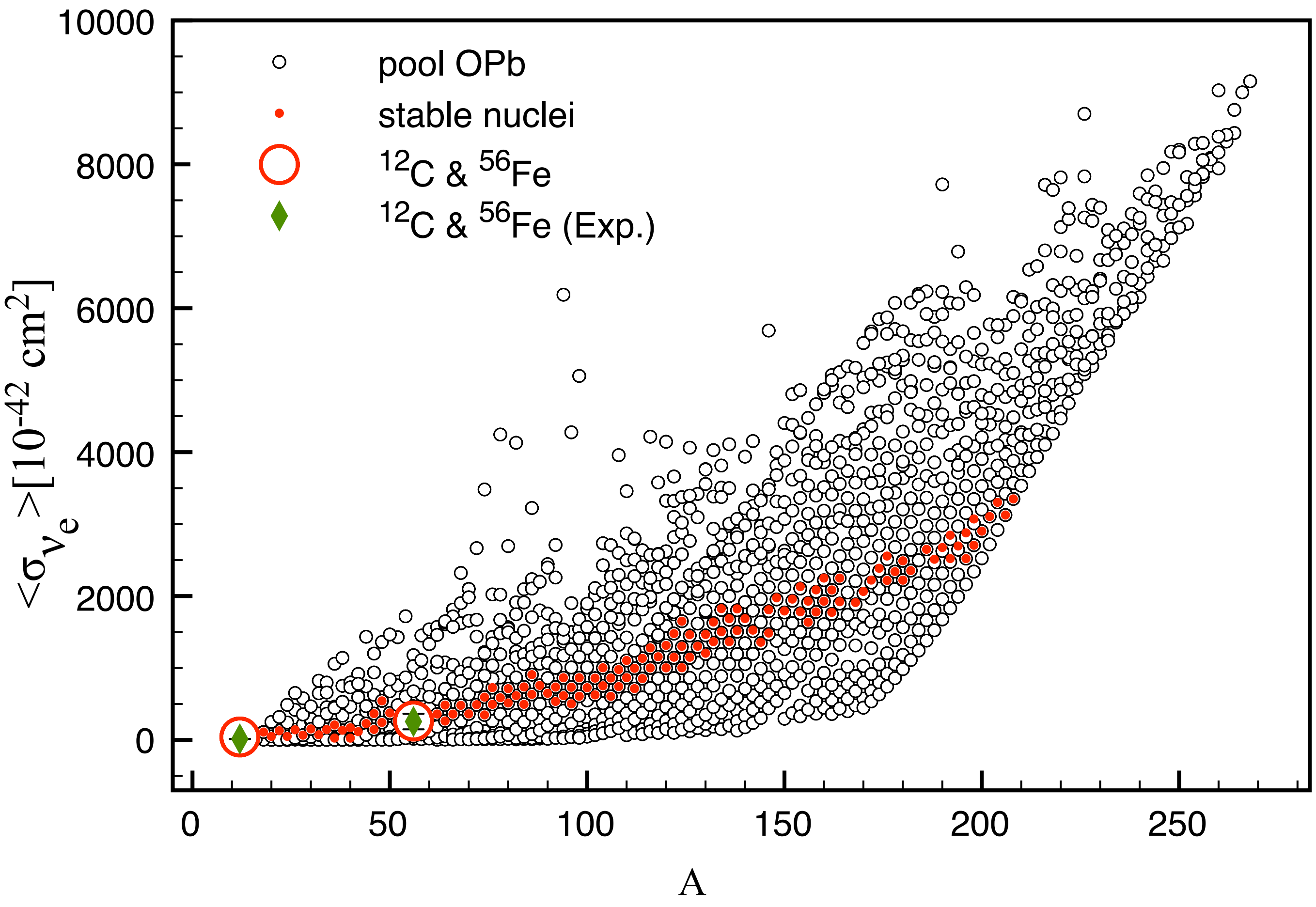

Model calculations include all multipoles (both parities) up to J=5.

The model calculations reasonably reproduce the only two experimental cases, ^{12}C and ^{56}Fe.

LARGE-SCALE CALCULATIONS OF ν-NUCLEUS CROSS SECTIONS

The cross sections averaged over supernova neutrino spectrum.

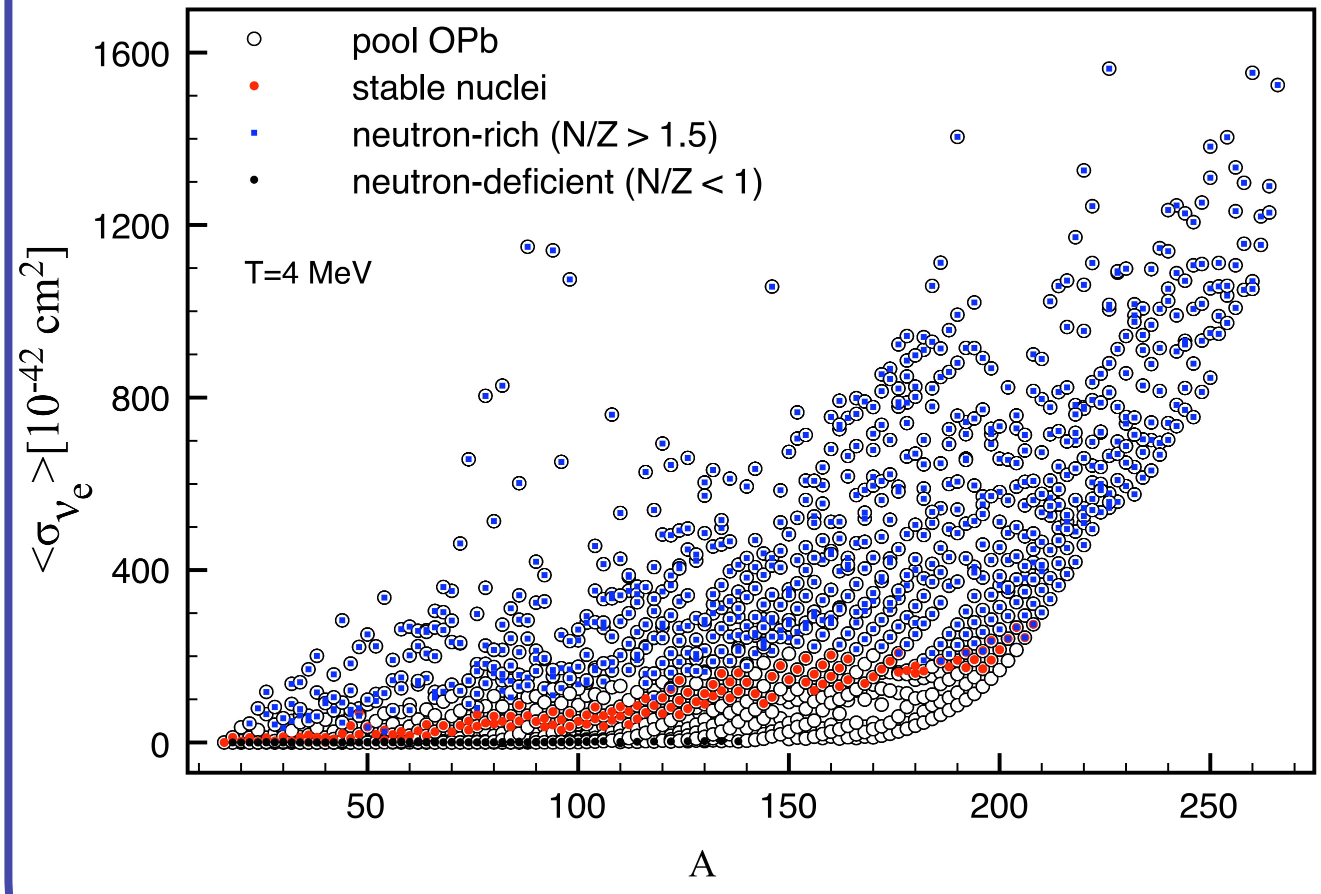

ADVANTAGES:

1) self-consistent parameter-free microscopic description of the cross sections (apart from the effective interactions that are fixed)

2) Complete calculations including all transition operators at finite momentum transfer and transitions up to J=5 (both parities)

The cross sections become considerably enhanced in neutron-rich nuclei, while those in neutron-deficient and proton-rich nuclei are small (blocking).

LARGE-SCALE CALCULATIONS OF ν-NUCLEUS CROSS SECTIONS

How the RNEDF results (up to J=5) compare to
ETFSI+CQRPA (only IAS & GT transitions; Borzov, Goriely) ?

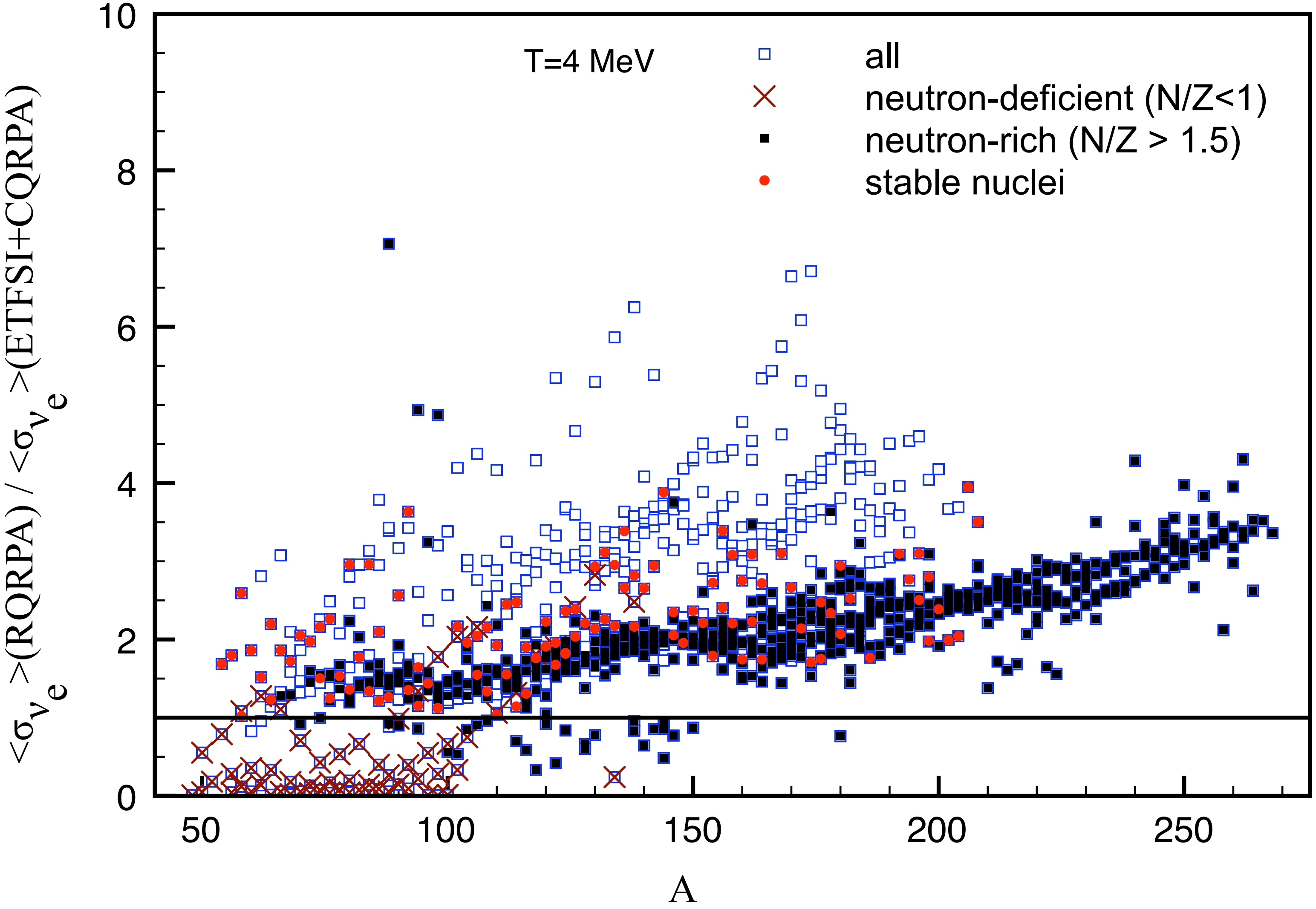

LARGE-SCALE CALCULATIONS OF ν-NUCLEUS CROSS SECTIONS

How the RNEDF results compare to RPA (Woods-Saxon + Landau-Migdal Force) by Kolbe, Langanke et al. ?

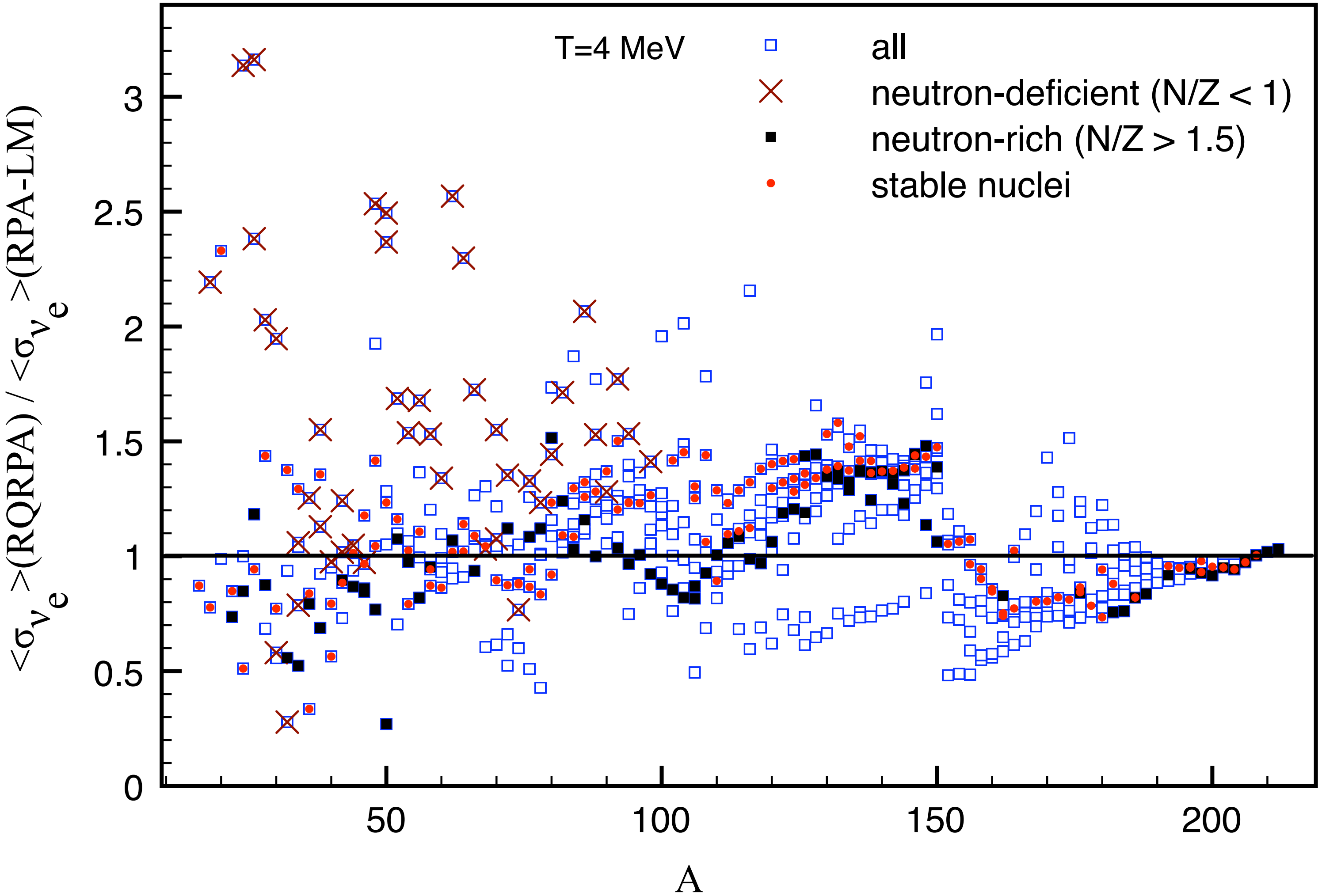

NEUTRAL-CURRENT NEUTRINO-NUCLEUS CROSS SECTIONS

- Inelastic neutrino-nucleus scattering through the weak neutral-current plays important role in neutrino transport in stellar environment

$$\nu_e +_Z X_N \rightarrow \nu_e +_Z X_N^*$$

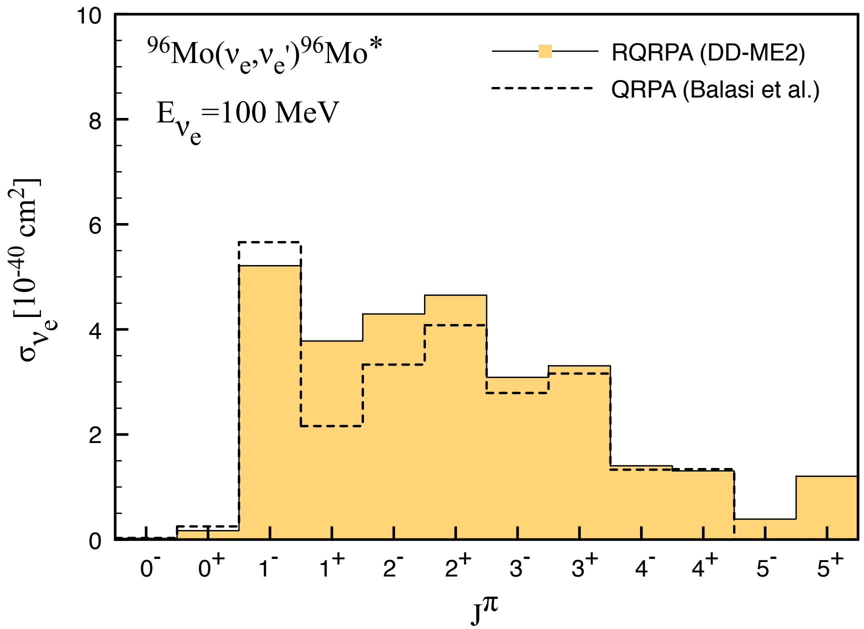

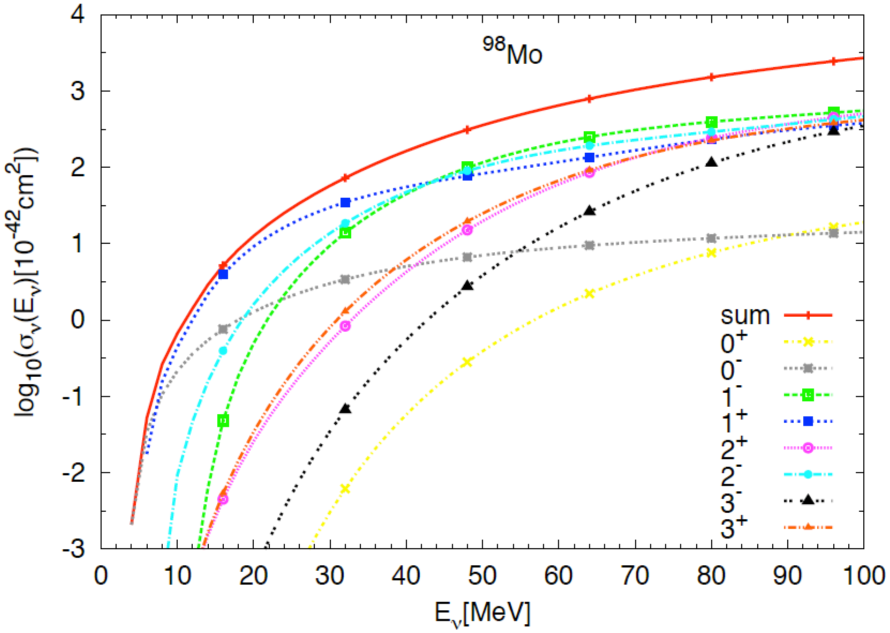

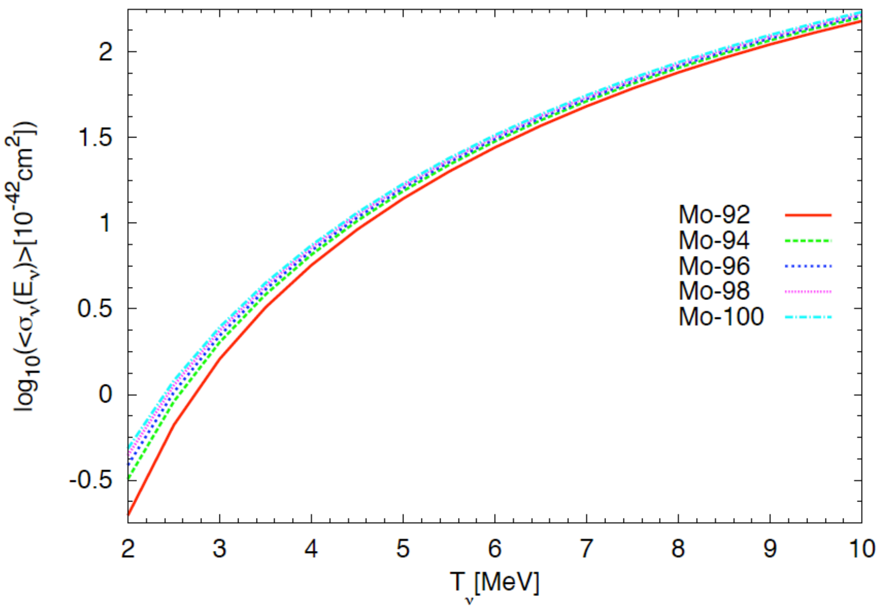

STELLAR ELECTRON CAPTURE

- The core of a massive star at the end of hydrostatic burning is stabilized by electron degeneracy pressure (as long as its mass does not exceed the Chandrasekhar limit)

- Electron capture reduces the number of electrons available for pressure support (in opposition to nuclear beta decay)

Electron capture

$$e^- +_Z X_N \rightarrow_{Z-1} X^*_{N+1} + \nu_e$$

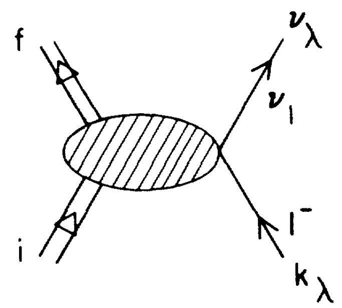

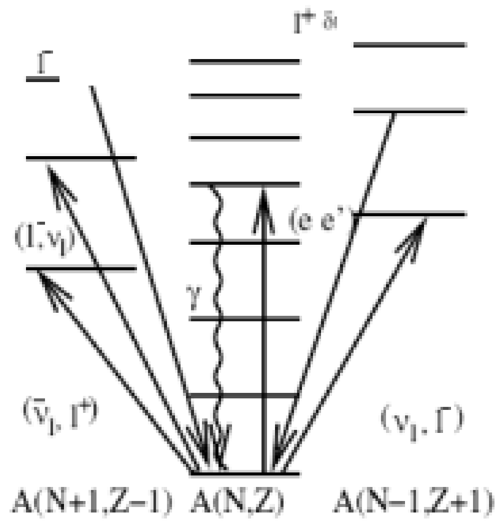

- Electron capture initiates the gravitational collapse of the core of a massive star, triggering a supernova explosion

ELECTRON CAPTURE (EC) CROSS SECTIONS

- Model based on finite temperature (RMF + RPA)

Finite temperature effects are described by Fermi-Dirac occupation factors for each single-nucleon state at the level of RMF, the same occupation factors are transferred to the RPA

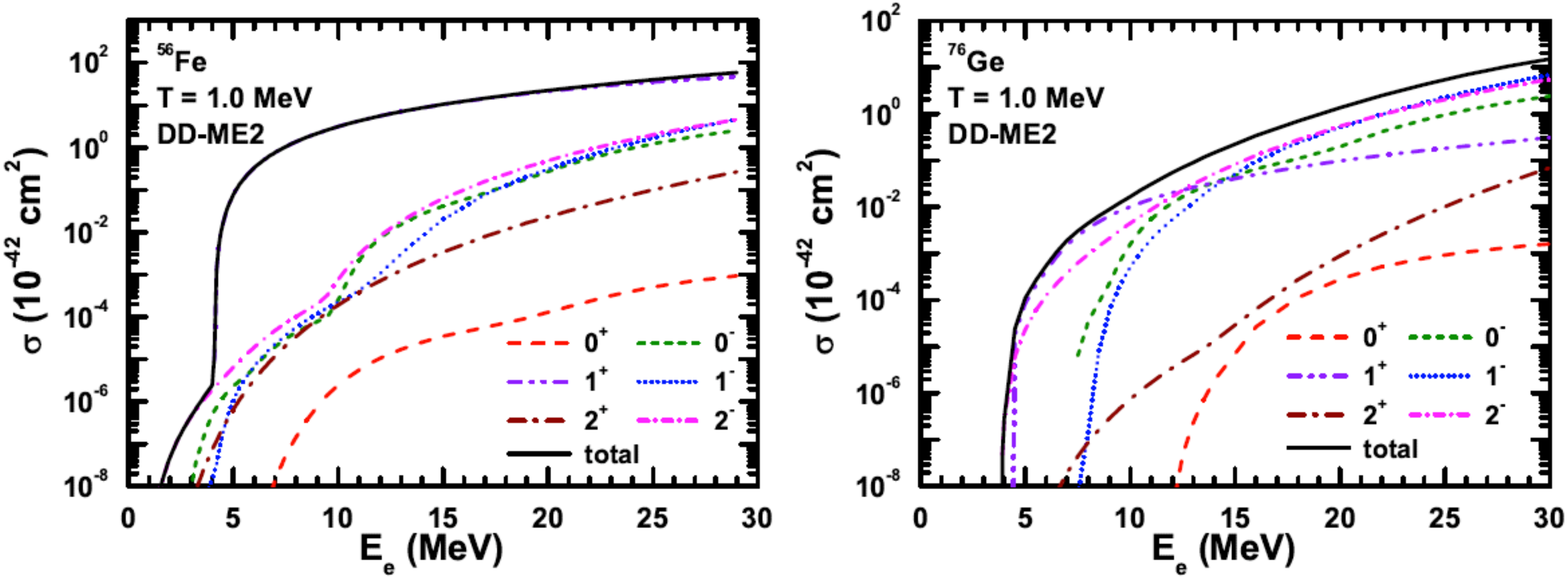

For ^{56}Fe the electron capture is dominated by the GT+ transitions, while for neutron-rich nuclei (^{76}Ge) forbidden transitions play more prominent role)

STELLAR ELECTRON CAPTURE ON NEUTRON RICH Ge ISOTOPES

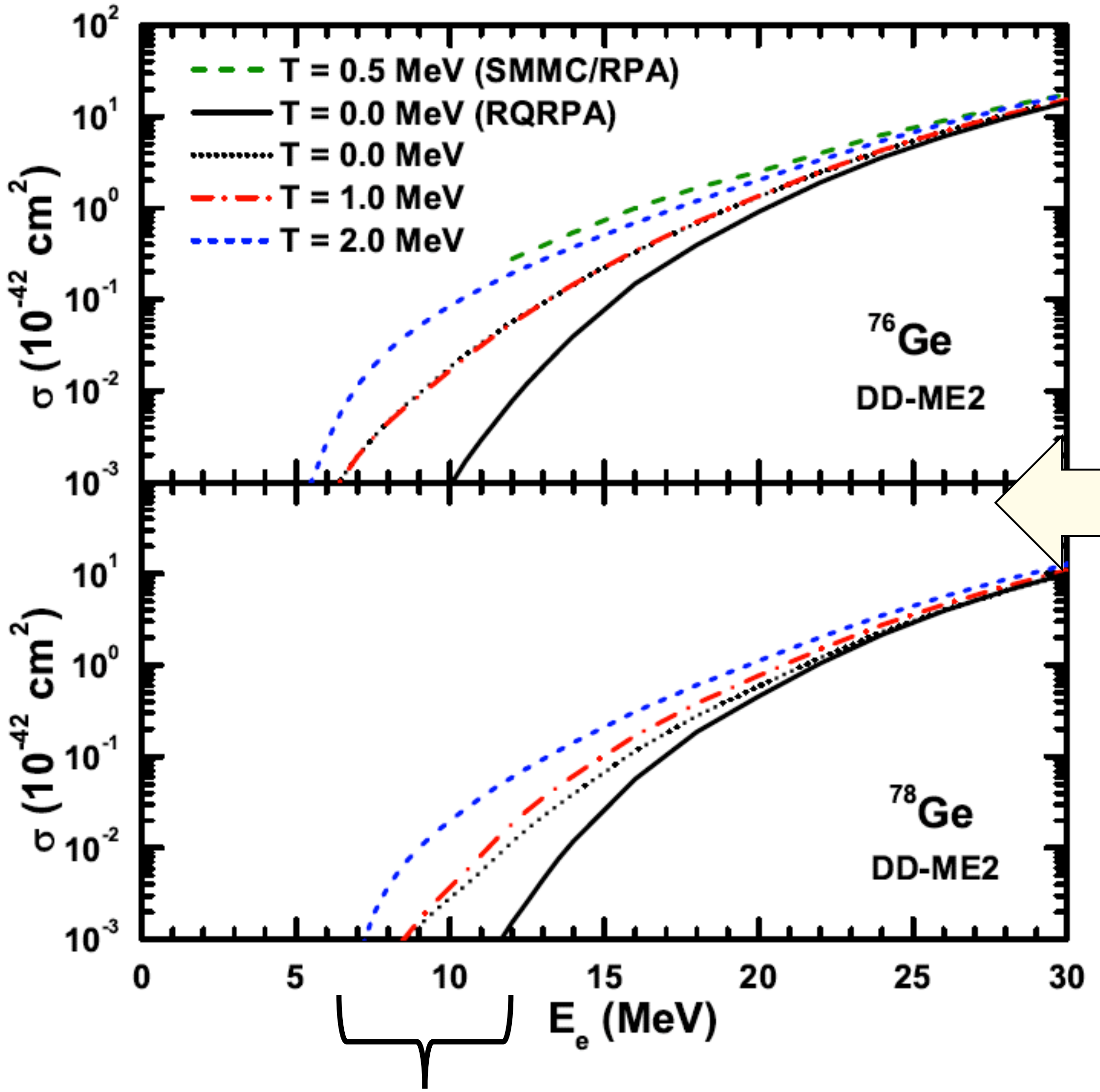

DEPENDENCE OF THE ELECTRON CAPTURE CROSS SECTIONS ON TEMPERATURE

Unblocking effect: electron-capture threshold energy decreases with temperature.

STELLAR ELECTRON CAPTURE RATES ON Fe ISOTOPES

$$\lambda_{\text{ec}} = \frac{1}{\pi^2 \hbar^3} \int_{E_e^0}^{\infty} p_e E_e \sigma_{ec}(E_e) f(E_e, \mu_e, T) dE_e$$

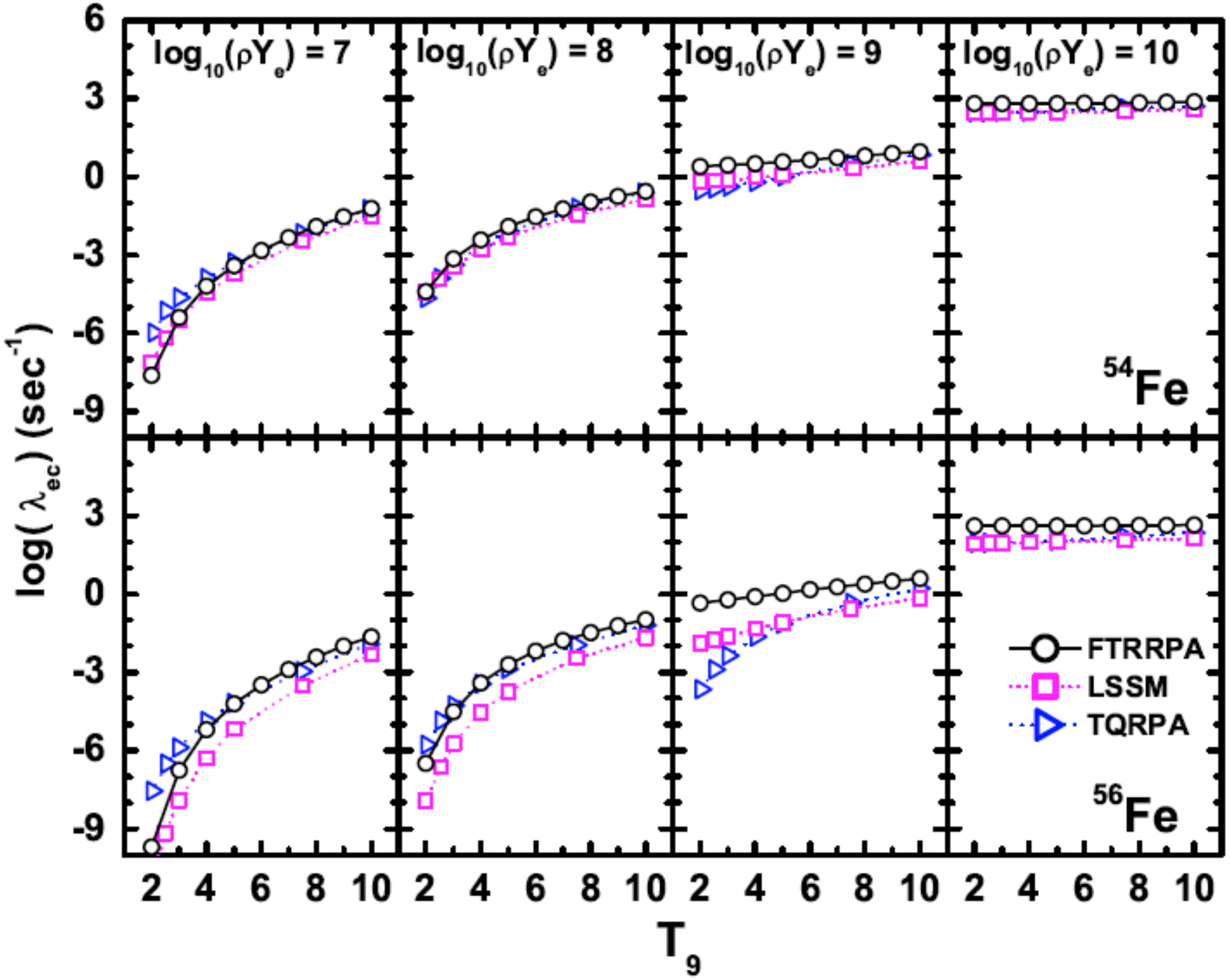

FTRRPA - present

LSSM – large scale shell model

K. Langanke and G. Martınez-Pinedo, At. Data Nucl. Data Tables 79, 1 (2001).

TQRPA

A.A. Dzhioev et al., PRC 81, 015804 (2010)

NUCLEAR EOS - CONSTRAINING THE SYMMETRY ENERGY

In order to explore the evolution of the excitation spectra as a function of the density dependence of the symmetry energy, a set of interactions is used, that span a broad range of values for the symmetry energy at saturation density (J) and the slope parameter (L).

Nuclear matter energy per part.:

$$E(\rho, \alpha) = E(\rho, 0) + S_2(\rho)\alpha^2 + \dots$$

$$\alpha = (N - Z)/A$$

Symmetry energy term:

$$S_2(\rho) = J - L\epsilon + \dots$$

$$\epsilon = (\rho_0 - \rho)/(3\rho_0)$$

$$L = 3\rho_0 \frac{dS_2(\rho)}{dr}|_{\rho_0}$$

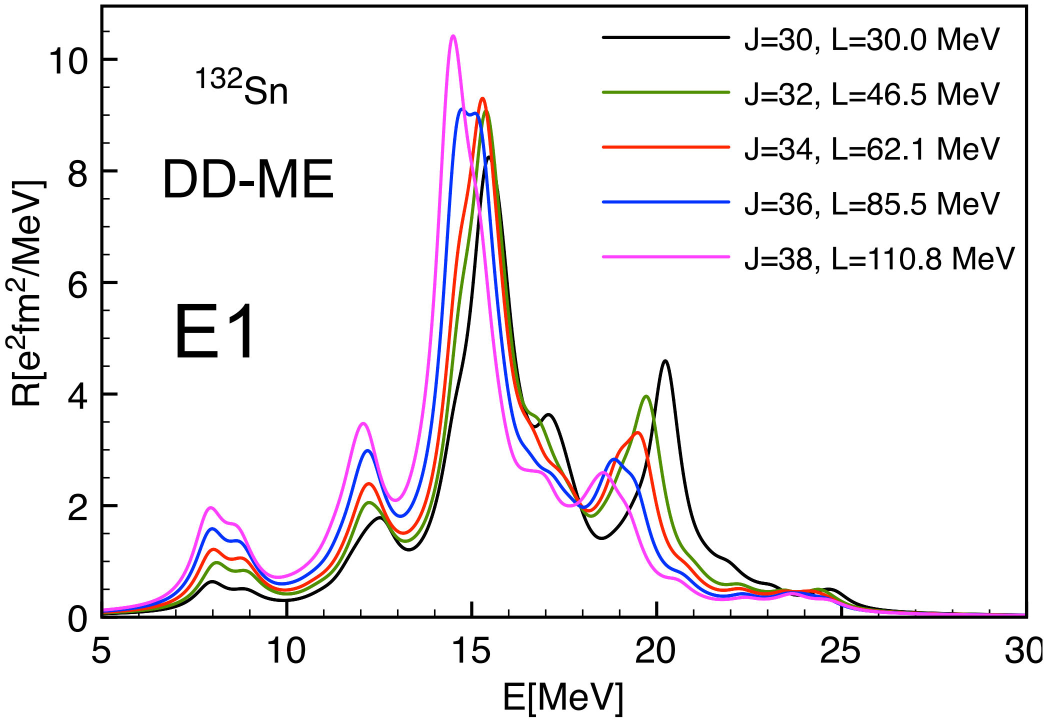

Neutron skin thickness (ΔR_{pn}) in nuclei is strongly correlated with symmetry energy at saturation density (J) & slope of the symmetry energy (L)

CONSTRAINING THE SYMMETRY ENERGY

• Theoretical constraints on the symmetry energy at saturation density [J] and slope of the symmetry energy [L] from dipole polarizability [$\alpha_D=(8\pi/9)e^2m_{-1}$] using relativistic nuclear energy density functionals

+

• Exp. data from polarized proton inelastic scattering, α_D=18.9(13)fm^3/e^2
A. Tamii et al., PRL. 107, 062502 (2011)

=

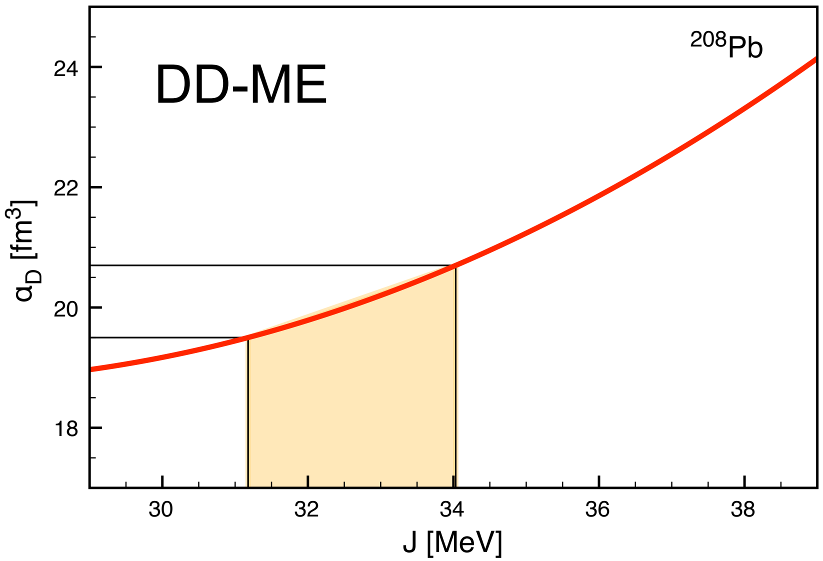

J=(32.6±1.4) MeV

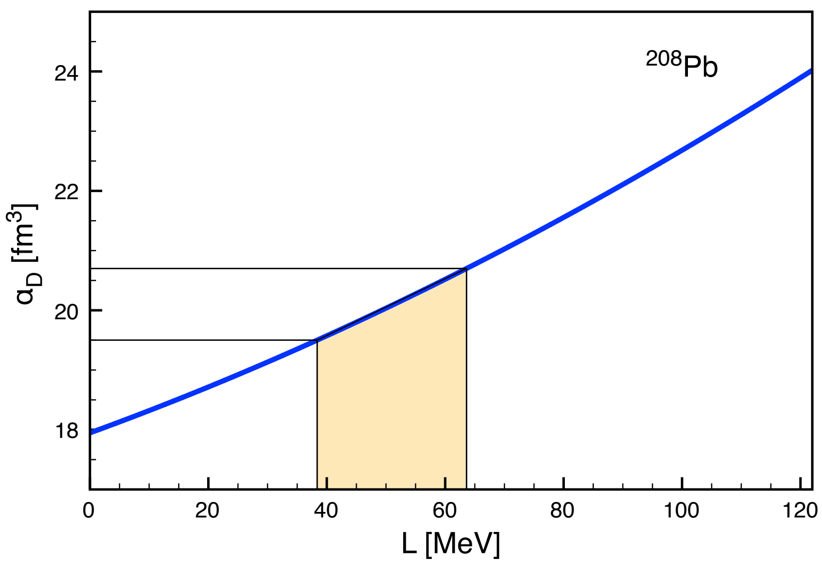

L=(50.9±12.6) MeV

CONSTRAINING THE SYMMETRY ENERGY

• Constraining the symmetry energy at saturation density (J) and slope of the symmetry energy (L) from various approaches:

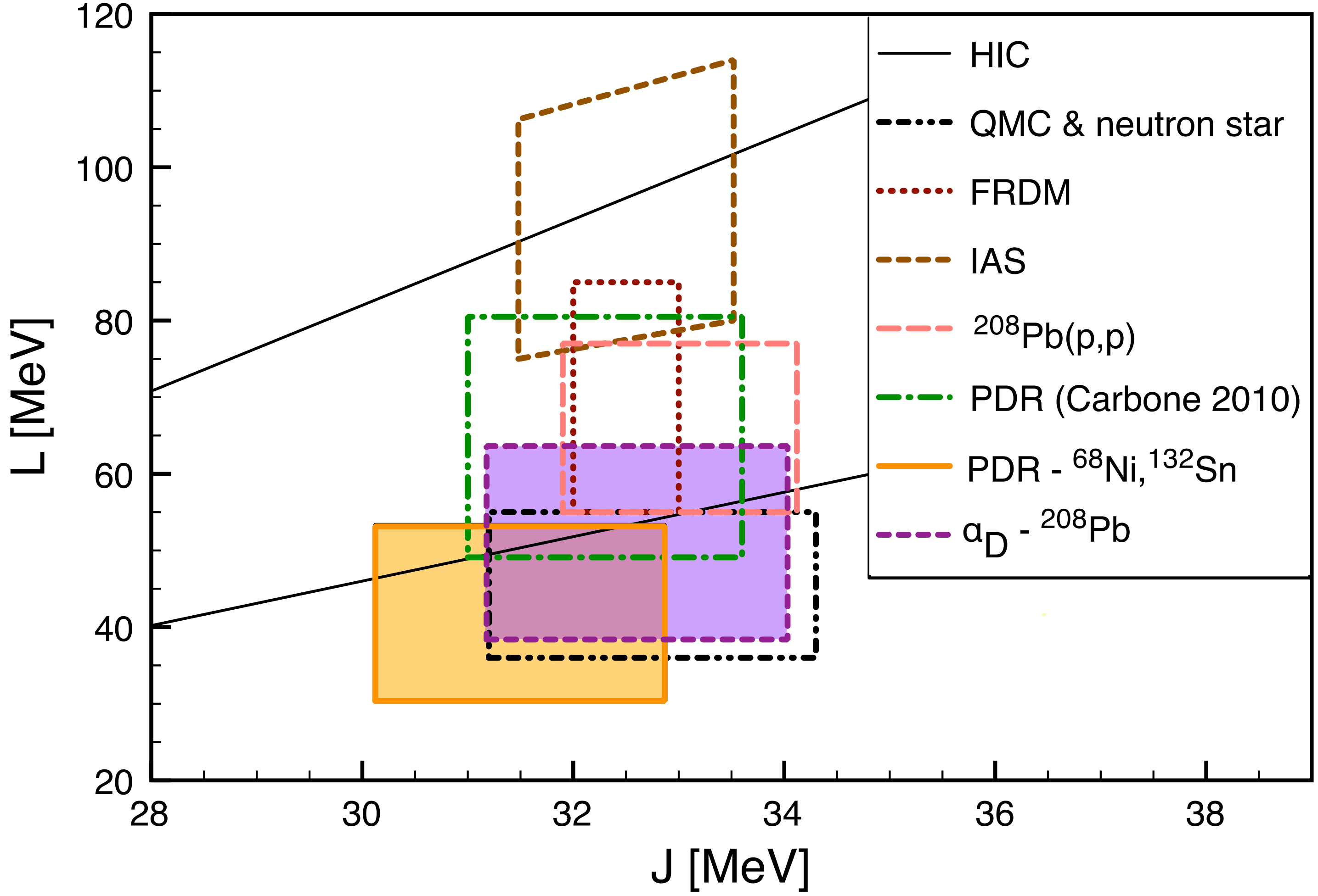

Also see M. B. Tsang et al., PRC 86, 015803 (2012)

ANTI-ANALOG GDR AND NEUTRON-SKIN THICKNESS

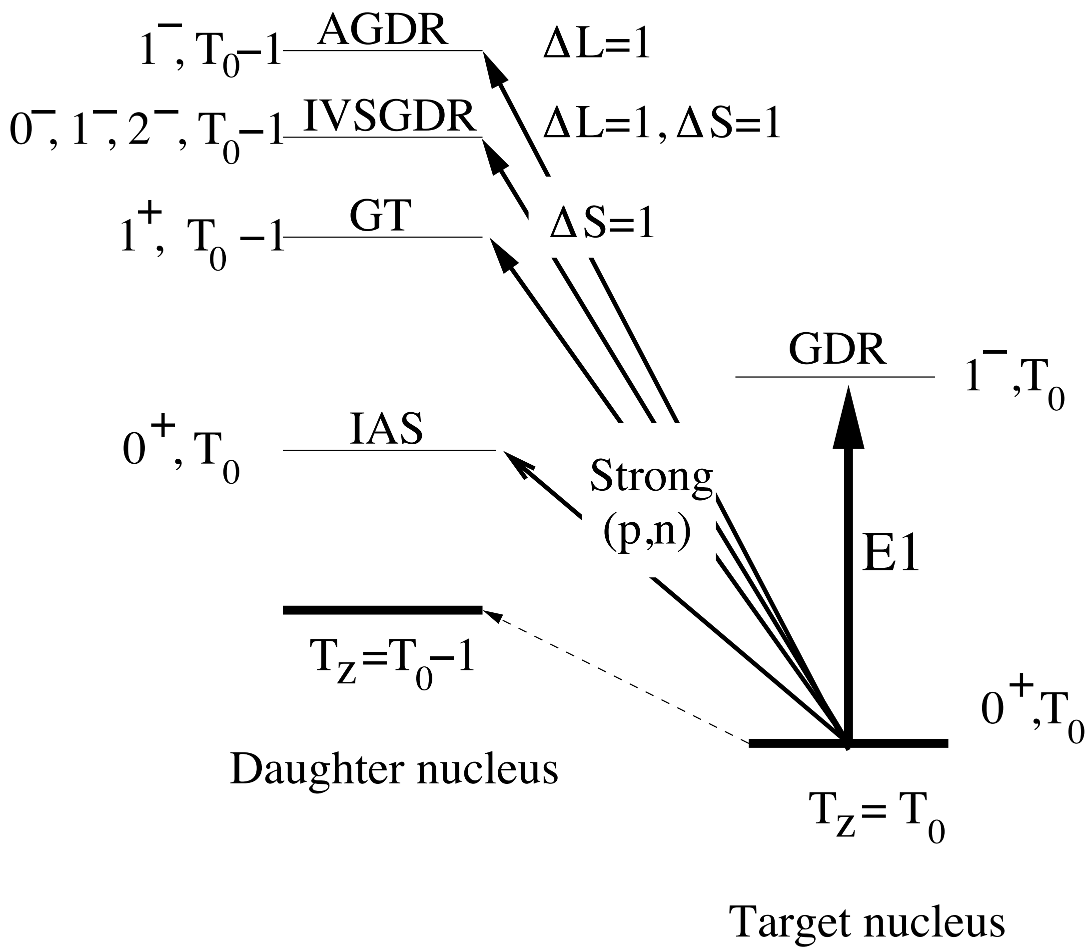

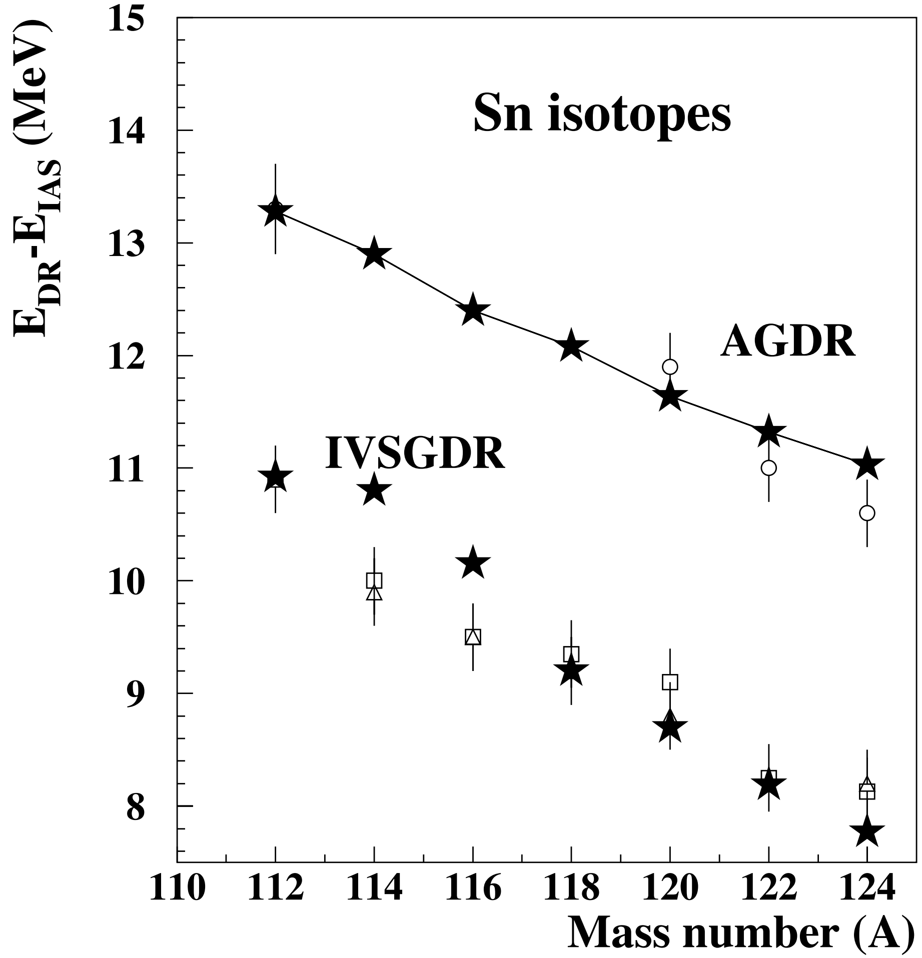

ANTI-ANALOG GDR AND NEUTRON-SKIN THICKNESS

TEST CASE: ^{124}Sn

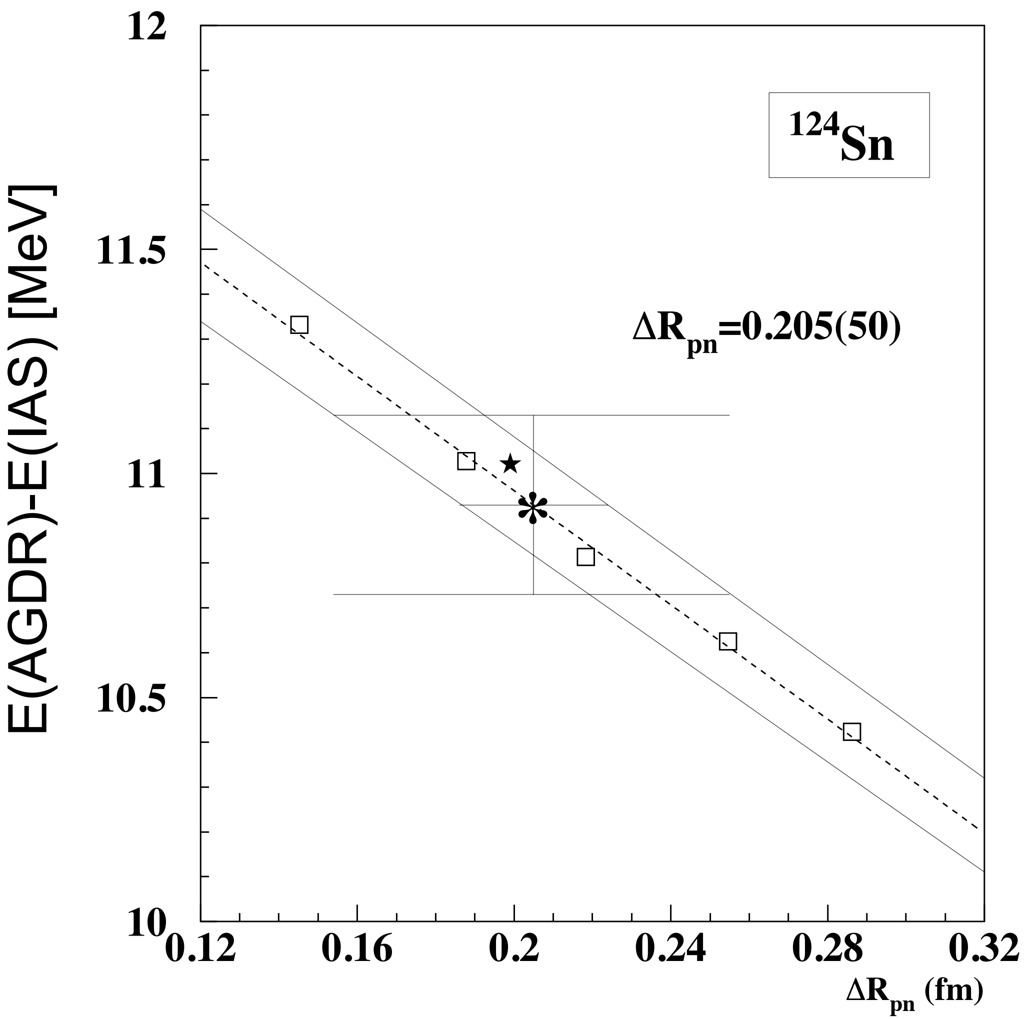

neutron skin thickness

METHOD	ΔR_{pn} (fm)
(p,p) 0.8 GeV	0.25 ± 0.05
(α,α') IVGDR 120 MeV	0.21 ± 0.11
Antiproton absorption	0.19 ± 0.09
(^{3}He,t) IVSGDR	0.27 ± 0.07
Pygmy dipole resonance	0.19 ± 0.05
(p,p) 295 MeV	0.185 ± 0.05
AGDR - present result	0.21 ± 0.05

CONCLUDING REMARKS

- ✓ We have established self-consistent framework based on the relativistic nuclear energy density functional to describe
  - neutrino-nucleus cross sections, both for neutral-current and charged current reactions
  - electron capture rates at finite temperature
- ○ Includes complete set of transition operators and transitions of all relevant multipoles (forbidden transitions)
- ○ This framework allows universal modeling of neutrino-nucleus cross sections (OPb pool completed), electron capture rates, and beta decays
- ✓ Studies (both theoretical and experimental) of dipole polarizability and AGDR provide useful constraints on the nuclear symmetry energy and neutron skin thickness

ACKNOWLEDGEMENTS & PUBLICATIONS

NEUTRINO-NUCLEUS REACTIONS:

- N. Paar, T. Suzuki, M. Honma, T. Marketin, and D. Vretenar, PRC 84, 047305 (2011).
- A. R. Samana, F. Krmpotic, N. Paar, C. A. Bertulani, PRC 83, 045807 (2011).
- H. Đapo, N. Paar, PRC 86, 035804 (2012).
- N. Paar, H. Tutman, T. Marketin, T. Fischer, submitted to PRC (2012).

ELECTRON CAPTURE:

- Y. F. Niu, N. Paar, D. Vretenar, and J. Meng, PRC 83, 045807 (2011).
- A. F. Fantina, E. Khan, G. Colo, N. Paar, and D. Vretenar, PRC 86, 035805 (2012).

NEUTRON-SKIN THICKNESS & SYMMETRY ENERGY:

- J. Piekarewicz et al., PRC 85, 041302(R) (2012).
- A. Krasznahorkay, N. Paar, D. Vretenar, M. Harakeh, submitted to PLB (2012).

GAMOW-TELLER TRANSITION STRENGTH FOR ^{56}Fe

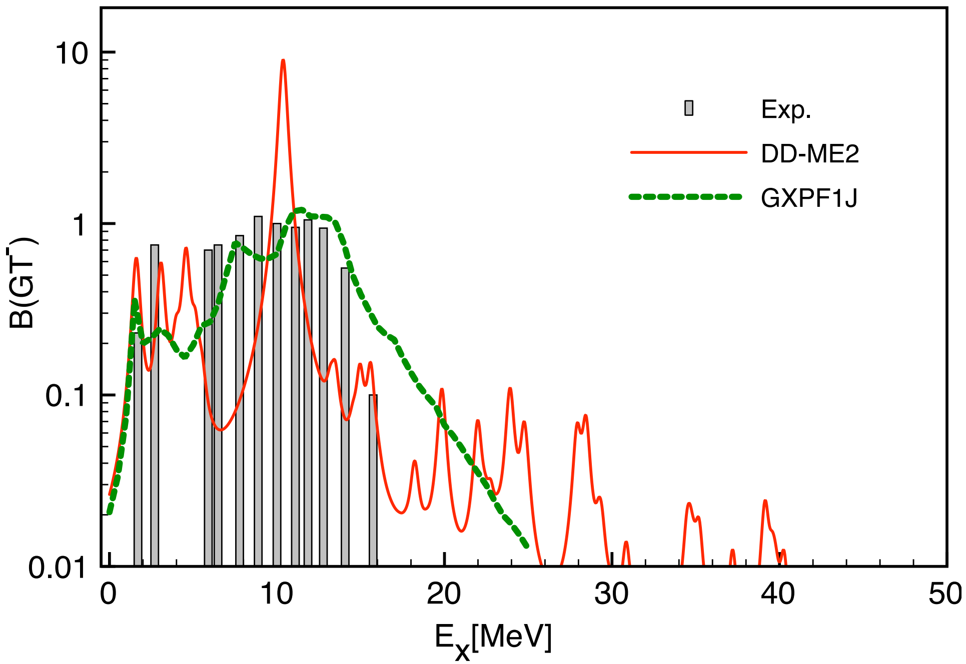

Gamow-Teller (GT) transitions calculated in two models:

- RQRPA (DD-ME2)
- Shell model (GXPF1J)
T. Suzuki et al.

Shell model includes important correlations among nuclei, accurately reproduces the experimental GT strength. However, already in medium mass nuclei the model spaces become large, many nuclei and forbidden transitions remain beyond reach.

RQRPA reproduces total GT strength and global properties of transition strength. Allows systematic calculations of high multipole excitations (forbidden transitions), enables extrapolations toward nuclei away from the valley of stability.